

TECHNICAL ADVANCE

Minitags for small molecules: detecting targets of reactive small molecules in living plant tissues using 'click chemistry'

Farnusch Kaschani¹, Steven H. L. Verhelst^{2,†}, Paul F. van Swieten³, Martijn Verdoes³, Chung-Sing Wong³, Zheming Wang^{1,4}, Markus Kaiser⁴, Herman S. Overkleeft³, Matthew Bogoy² and Renier A. L. van der Hoorn^{1,4,*}

¹Plant Chemetics Lab, Chemical Genomics Centre of the Max Planck Society, Max Planck Institute for Plant Breeding Research, Carl-von-Linné-Weg 10, 50829 Cologne, Germany,

²Department of Pathology, Stanford University School of Medicine, 300 Pasteur Drive, Stanford, 94305 California, USA,

³Leiden Institute of Chemistry, Leiden University, PO Box 9502, 2300 RA Leiden, The Netherlands, and

⁴Chemical Genomics Centre of the Max Planck Society, Otto-Hahn-Strasse 15, 44227 Dortmund, Germany

Received 5 August 2008; revised 1 September 2008; accepted 3 September 2008; published online 27 October 2008.

*For correspondence (fax +49 221 50 62 207; e-mail hoorn@mpiz-koeln.mpg.de).

[†]Present address: Chemie der Biopolymere, Technical University Munich, Weihenstephanerberg 3, Freising, 85354, Munich, Germany.

Summary

Small molecules offer unprecedented opportunities for plant research since plants respond to, metabolize, and react with a diverse range of endogenous and exogenous small molecules. Many of these small molecules become covalently attached to proteins. To display these small molecule targets in plants, we introduce a two-step labelling method for minitagged small molecules. Minitags are small chemical moieties (azide or alkyne) that are inert under biological conditions and have little influence on the membrane permeability and specificity of the small molecule. After labelling, proteomes are extracted under denaturing conditions and minitagged proteins are coupled to reporter tags through a 'click chemistry' reaction. We introduce this two-step labelling procedure in plants by studying the well-characterized targets of E-64, a small molecule cysteine protease inhibitor. In contrast to biotinylated E-64, minitagged E-64 efficiently labels vacuolar proteases *in vivo*. We displayed, purified and identified targets of a minitagged inhibitor that targets the proteasome and cysteine proteases in living plant cells. Chemical interference assays with inhibitors showed that MG132, a frequently used proteasome inhibitor, preferentially inhibits cysteine proteases *in vivo*. The two-step labelling procedure can be applied on detached leaves, cell cultures, seedlings and other living plant tissues and, when combined with photoreactive groups, can be used to identify targets of herbicides, phytohormones and reactive small molecules selected from chemical genetic screens.

Keywords: click chemistry, small molecule, E-64, papain-like cysteine protease, proteasome, MG132.

Introduction

Plants respond to, metabolize and produce a diverse range of small molecules. Examples are plant hormones (e.g. auxin, gibberellic acid and salicylic acid), secondary metabolites and exogenous small molecules like herbicides or growth regulators or compounds identified from animal research or from screening chemical libraries (reviewed by Kaschani and Van der Hoorn, 2007). Other small molecules are metabolized and used to modify and regulate protein activities. These small molecules offer unprecedented

opportunities for plant research. However, to understand their mechanism of action, it is essential to monitor the location of small molecules in plants and identify their targets.

With the help of reporter tags like biotin (for affinity purification) or rhodamine (for fluorescence imaging) it is possible to detect, localize and analyse potential targets of small molecules. However, large reporter tags can disturb the specificity of small molecules, and labelling with biotin-

or rhodamine-labelled small molecules is frequently limited to *in vitro* work with protein extracts since the relatively large reporter tags limit the membrane permeability.

To study the fate of small molecules that react covalently with their targets without disturbing their availability or specificity, a two-step labelling approach can be used (Figure 1a) (Speers and Cravatt, 2004). In step 1, labelling is achieved with small molecules that are tagged with a miniature membrane-permeable chemical tag, based on the azide (N_3 , 41 Da) or alkyne (\equiv , 24 Da) functional group. These chemical tags are very stable under biological conditions (Wang *et al.*, 2003). In step 2, after labelling, proteins are extracted and azide- or alkyne-labelled proteins are coupled to an alkyne- or azide-modified reporter tag, respectively, through a so-called 'click chemistry' reaction (Kolb *et al.*, 2001; Figure 1b). This organic chemistry reaction is highly specific ('bio-orthogonal') and is based on the Cu^{1+} -catalysed Huisgen's 1,3-dipolar cycloaddition (Huisgen, 1984; Rostovtsev *et al.*, 2002; Tornøe *et al.*, 2002). Speers and Cravatt (2004) used this two-step labelling procedure to identify targets of azide- and alkyne-labelled phenyl sulphamate probes in living mice.

To broaden its application to other small molecules and other organisms, we established and validated the two-step labelling procedure using the well-characterized targets of the small molecule E-64. E-64 is a mechanism-based inhibitor that specifically and irreversibly reacts with papain-like

cysteine proteases in an activity-dependent manner (Powers *et al.*, 2002). We previously showed that a biotinylated version of E-64, DCG-04 (Greenbaum *et al.*, 2000), biotinylates six different papain-like cysteine proteases in Arabidopsis leaf extracts (Van der Hoorn *et al.*, 2004). The identified proteases included the vacuolar Arabidopsis aleurain-like protease (AALP, Ahmed *et al.*, 2000) and the vesicle-localized drought-induced protease RD21 (Hayashi *et al.*, 2001). In this study we used E-64 and its known targets to establish the parameters for two-step *in vivo* labelling, and used this optimized protocol to study *in vivo* labelling by minitagged E-64 and a minitagged proteasome probe. The two-step labelling procedure is simple, versatile and robust, and will facilitate the detection and identification of other small-molecule targets in plants.

Results

An optimal coupling protocol

In order to extend and demonstrate the utility of *in vivo* labelling we synthesized a set of novel E-64 derivatives, called N_3Le , N_3YLe , $\equiv Le$ and $\equiv YLe$ (Figure 2). All carry an epoxide (e) reactive group and a leucine (L) which is preferred at the P2 position of substrates by papain-like cysteine proteases. Some carry a tyrosine linker (Y), added for proper comparison with DCG-04. E-64 derivatives that carry an azide function (N_3) can be coupled to biotin-alkyne (Bio \equiv), whereas alkyne (\equiv) derivatives can be coupled to biotin-rhodamine-azide (BioRh N_3) (Figure 2).

The coupling of the azide and alkyne moieties is achieved by Huisgen's 1,3-dipolar cycloaddition, which occurs bio-orthogonally at room temperature and is catalysed by Cu^{1+} (Figure 1b). Cu^{1+} is not stable and has to be generated *in situ* by reduction of Cu^{2+} . Speers and Cravatt (2004) achieved this reaction with the reducing agent 2-amino-2-(hydroxymethyl)-1,3-propanediol (TRIS)-(2-carboxyethyl)phosphine (TCEP) and stabilized Cu^{1+} using TRIS-(benzyltriazolylmethyl)amine (TBTA) as a ligand (Chan *et al.*, 2004). We developed a protocol without TBTA, using DTT as reducing agent (see Experimental Procedures). The coupling buffer is composed of 0.4 mM DTT, 50 mM sodium acetate (NaOAc) (pH 6), 1 mM $CuSO_4$, 1% SDS and 6–10 μM of the respective azide- or alkyne-modified reporter tag. We also include an acetone precipitation before coupling to standardize the reaction conditions for the coupling reaction.

We first demonstrate that the coupling reaction is specific within a plant proteome. Arabidopsis leaf extracts were labelled with DCG-04 or N_3YLe *in vitro*, and N_3YLe -labelled proteomes were treated with coupling buffer containing Bio \equiv (Figure 3a). Signals generated by two-step labelling with $N_3YLe/Bio\equiv$ are comparable with those generated by labelling with DCG-04 with signals at 40, 30 and 25 kDa, indicated with dots in the figures

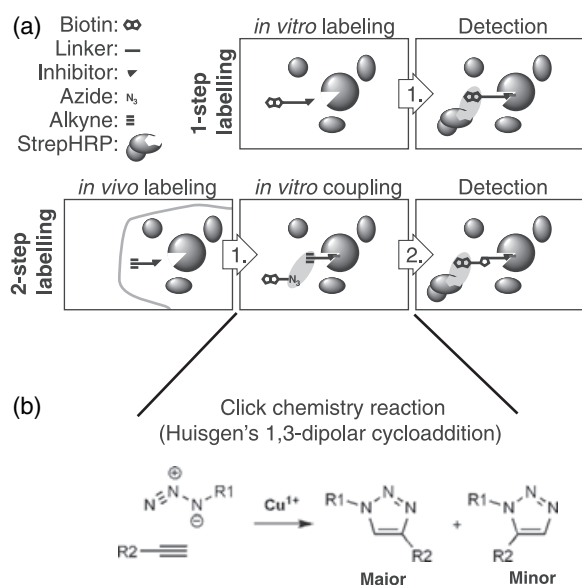


Figure 1. Principle of one-step and two-step labelling.

(a) Comparison of one-step and two-step labelling. The approaches differ experimentally by one additional coupling step.

(b) Schematic representation of the click chemistry reaction. Molecules carrying an azide group are coupled to terminal alkynes via Huisgen's 1,3-dipolar cycloaddition resulting in a stable triazole moiety. The Cu^+ -catalysed reaction is performed at room temperature and is highly specific (Wang *et al.*, 2003).

Figure 2. Structures of E-64-based probes (top) and biotinylated tags (bottom).

\equiv Le, \equiv YLe, N_3 Le and N_3 YLe are derivatives of E-64 carrying leucine (L) and tyrosine (Y) in the linker next to the epoxide (e) reactive group and an alkyne (\equiv) or azide (N_3) as the chemical minitag. Bio \equiv and BioRh N_3 are the corresponding reporter tags containing biotin (Bio) and rhodamine (Rh).

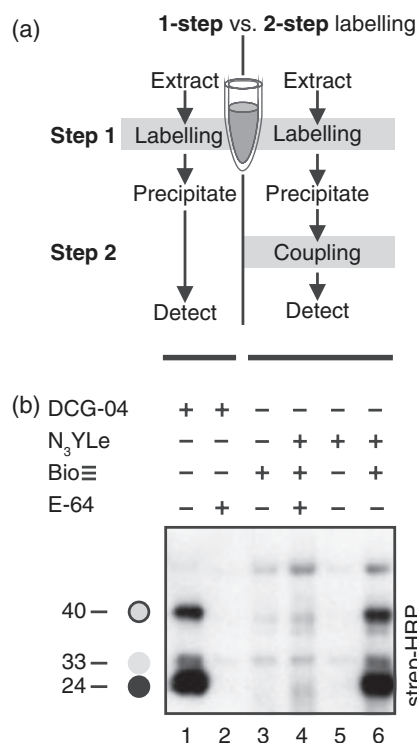
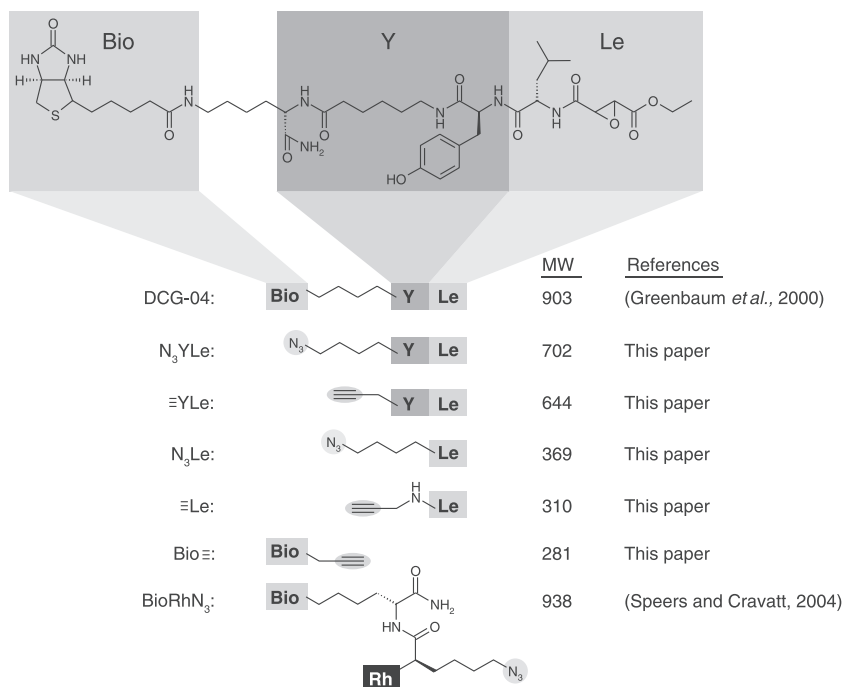


Figure 3. Comparison of one-step with two-step labelling.

(a) Schematic representation of the practical steps involved in one-step and two-step *in vitro* labelling.

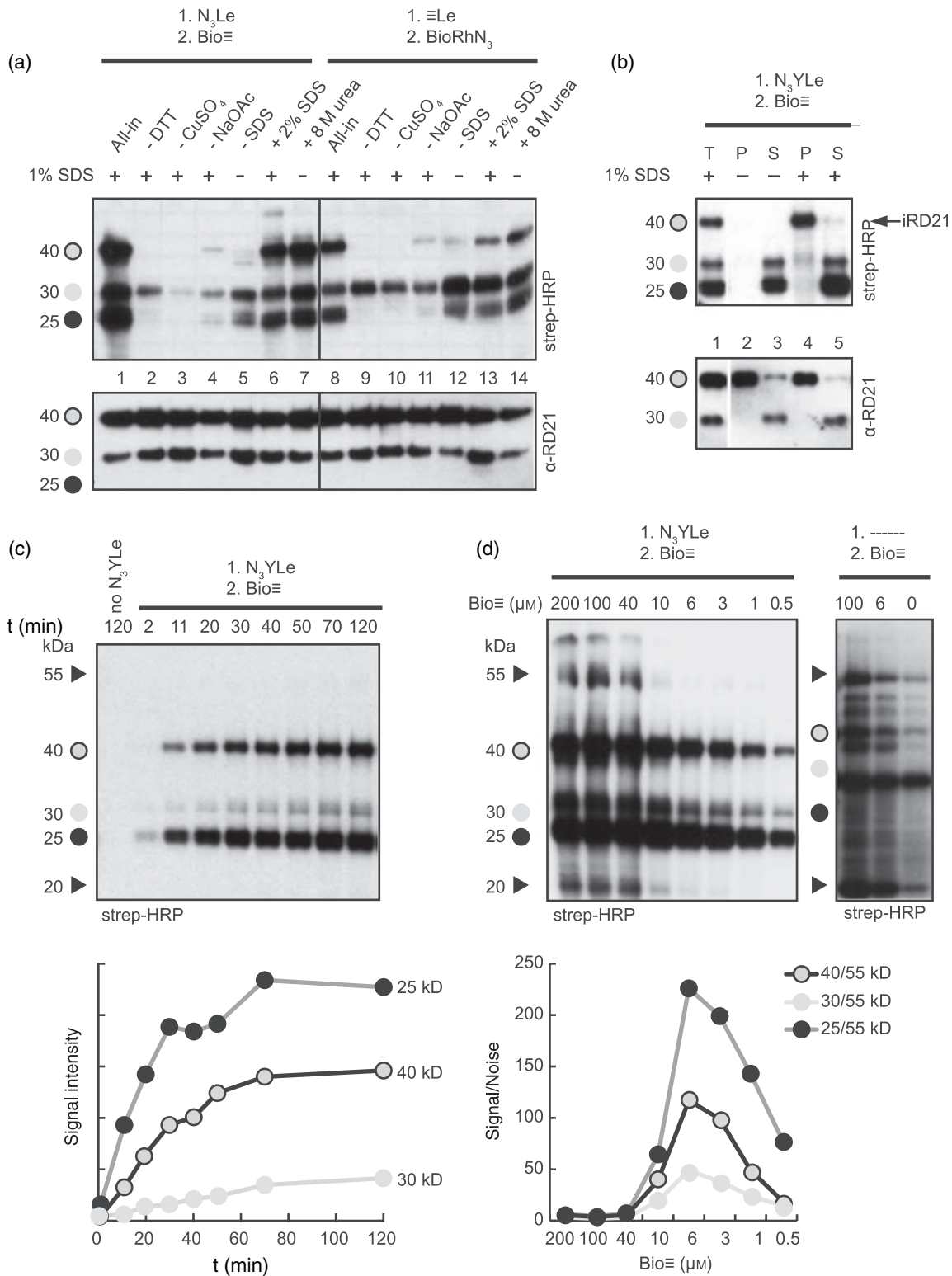
(b) One-step and two-step *in vitro* labelling of papain-like cysteine proteases in Arabidopsis leaf extracts. The result of both approaches is similar (lanes 1 and 6). Concentrations used: 2 μ M DCG-04; 5 μ M N_3 YLe; 6 μ M Bio \equiv ; 100 μ M E-64. All samples were treated the same way except for the components indicated on top. Proteins were separated on protein gels, transferred to protein blots and detected with streptavidin-horseradish peroxidase (HRP).

(Figure 3b, lanes 1 and 6). Labelling can be completed by adding an excess of E-64, indicating that the labelling is specific (Figure 3b, lanes 2 and 4). Furthermore, the signals are not observed if Bio \equiv is omitted from the coupling buffer, whereas omitting N_3 YLe from labelling results in low background signals (Figure 3b, lanes 3 and 5). The data demonstrate a low level of unspecific labelling, illustrating the specificity of click chemistry reactions within plant proteomes.

The two-step labelling can be done in two ways: alkyne-E-64 plus azide-biotin or azide-E-64 plus alkyne-biotin. Both procedures result in the same signals (Figure 4a, lanes 1 and 8), indicating that the chemical tag has no influence on the specificity of the probe. The signals are also identical with those generated with N_3 YLe or \equiv YLe (Figure 3b and data not shown), indicating that the tyrosine linker (Y) has no influence on the reactivity and specificity of the probes *in vitro*.

Parameters for optimal coupling

We next showed the role of each of the components of the coupling reaction. Lack of DTT or $CuSO_4$ results in a complete loss of the expected signals (Figure 4a, lanes 2, 3, 9 and 10). Signal intensities are strongly reduced in the absence of the NaOAc buffer (Figure 4a, lanes 4 and 11). In the absence of SDS, the profile lacks a signal at 40 kDa (Figure 4a, lanes 5 and 12). We suspected that SDS has an effect on the solubility of the 40 kDa protein and not on the coupling reaction itself because the 25-kDa and 30-kDa signals are still visible. To test this hypothesis,



N_3 YLe-labelled protein samples were centrifuged and the supernatant separated from the pellet. Both fractions were then coupled to Bio \equiv in the absence and presence of 1% SDS. The 30-kDa and 25-kDa signals were detected in

both soluble fractions, indicating that the coupling reaction does not depend on SDS (Figures 4b, lanes 1 and 3). However, the 40-kDa signal is present in the pellet fraction and requires SDS for coupling with biotin (Figure 4b,

lanes 2 and 4). Previous work showed that the 40-kDa signal represents the intermediate isoform of RD21 (iRD21), an abundant cysteine protease in Arabidopsis leaf extracts (Van der Hoorn *et al.*, 2004; Yamada *et al.*, 2001). Western blotting with anti-RD21 antibodies shows that the 40-kDa iRD21 is indeed in the pellet fraction (Figure 4b, bottom). Taken together, the presence of SDS in the coupling buffer is not crucial for the coupling reaction itself but it helps to resolubilize precipitated proteins, making them available for coupling.

To ensure that labelling reflects *in vivo* conditions, extraction and coupling should be performed under denaturing conditions. We already showed that the coupling is compatible with 1% SDS (Figure 4a, lanes 1 and 8). We now tested whether the coupling reaction is compatible with 2% SDS or 8 M urea. Concentrations of SDS up to 2% and 8 M urea did not affect the coupling reaction (Figure 4a, lanes 6, 7, 13 and 14). Other detergents like Triton X-100 and Tween-20 were also tolerated but they were less effective in solubilizing the 40-kDa iRD21 (data not shown). Higher salt concentrations (up to 800 mM NaOAc) were tolerated but caused considerable unspecific labelling. Other buffer systems (TRIS buffer and phosphate buffer) and pH values from 4 to 8 were compatible with the coupling reaction, but pH 6 in 50 mM NaOAc was found to be optimal for coupling (data not shown). Overall these data demonstrate that this coupling protocol is versatile and robust. It tolerates many additives (detergents, urea, salts) and allows coupling under denaturing conditions which is essential when *in vivo* reactions are analysed.

We also tested different coupling times and reporter tag concentrations. A time course experiment shows that the coupling reaction occurs within 10 min and reaches its maximum within 60 min (Figure 4c). Extended coupling times, however, did not result in increased unspecific coupling (Figure 4c, compare first and last lanes). Coupling at different reporter tag concentrations shows that the optimal reporter tag concentration is 3–10 μM (Figure 4d). At lower concentrations the signal drops in intensity and at higher concentrations proteins become unspecifically

labelled with Bio \equiv (arrowheads in Figure 4d), even in the absence of azide-E64 (Figure 4d, right panel). These results illustrate that the amount of unspecific labelling during the coupling reaction can be controlled with optimized reporter tag concentrations.

In vivo labelling using the optimized two-step protocol

Having established two-step labelling with small untagged molecules *in vitro*, we could now investigate enzyme activities in living plant tissues (*in vivo*). Therefore, detached leaves were incubated with their petioles in a solution containing the probe (Figure 5a). After labelling, a leaf disc was taken from part of the leaf that did not contact the probe-containing solution. Proteins were extracted from this leaf disc under denaturing conditions to ensure that the signals reflect *in vivo* labelling. N₃Le-labelled proteins were coupled to Bio \equiv and analysed. The samples were taken from independent leaves to determine how reproducible two-step labelling is. The signals that are detected with N₃Le are similar to those detected *in vitro* with N₃Le (Figure 5b) and DCG-04 (Figure 3b). The intensity, however, is 10-fold higher for *in vivo* labelling when compared with *in vitro* labelling despite the same N₃Le concentration being used (Figure 5b, lanes 3–6). A N₃Le dilution series showed that the minimal probe concentration required for maximal *in vivo* labelling is 3–5 μM N₃Le (Figure 5c).

We next investigated the kinetics of N₃Le *in vivo* labelling and whether the biotinylated probe DCG-04 could generate the same signals *in vivo* as N₃Le. Therefore, leaves were incubated in DCG-04 and N₃Le for different time points and biotinylated proteins were generated and analysed as described above. Interestingly, 40- and 30-kDa proteins are labelled by N₃Le within 90 min, whereas the 25-kDa proteins are labelled in 120 min (Figure 5d). In contrast, *in vivo* DCG-04 labelling of both 40- and 30-kDa proteins reaches its maximum in 120 min (Figure 5e), but no 25-kDa protein is labelled. All signals are effectively competed *in vivo* by adding an excess of the membrane

Figure 4. Parameters of optimal coupling.

(a) N₃Le-labelled proteins (lanes 1–7) and \equiv Le-labelled proteins (lanes 8–14) were dissolved in coupling buffer ('All-in', lanes 1 and 8) or in coupling buffer either lacking one component (lanes 2–5 and 9–12) or 'All-in'-buffer supplemented with 2% SDS (lanes 6 and 13) or 8 M urea (lanes 7 and 14). Proteins were detected on membrane with streptavidin-HRP (top panel) and α -RD21 antibody (bottom panel). Dithiothreitol (DTT) and CuSO₄ are essential whereas lack of sodium acetate (NaOAc) results in less efficient coupling. Concentrations of SDS up to 2% and 8 M urea are tolerated during coupling. The signal remaining at 30 kDa is non-specific since it is also visible in the no probe control (Figure 3b, lane 3).

(b) Sodium dodecyl sulphate is essential to make precipitated proteins available for coupling. A N₃YLe-labelled protein extract (T) was centrifuged and the soluble fraction (S) was separated from the pellet (P) and precipitated with 100% acetone. Both fractions were coupled to Bio \equiv in the presence or absence of 1% SDS. The proteins were analysed as described in Figure 3(b). In the absence of SDS the N₃YLe-iRD21 conjugate (bottom panel, lane 2) is not available for coupling (top panel, lane 2).

(c) Time course of coupling. N₃YLe-labelled plant extracts were coupled for various times with 6 μM Bio \equiv . Signals were quantified and plotted against time. Coupling occurs within 10 min and reaches its maximum within 60 min.

(d) Coupling at different tag concentrations. N₃YLe-labelled plant extracts were coupled with different concentrations of Bio \equiv . At tag concentrations higher than 40 μM considerable unspecific labelling is observed (arrowheads upper panel). The intensities were measured at 25, 30 and 40 kDa ('signals') and at 55 kDa ('noise'). The signal-to-noise ratio was calculated for each of the signals (bottom graph). The signal-to-noise ratio is optimal between 3 and 10 μM Bio \equiv .

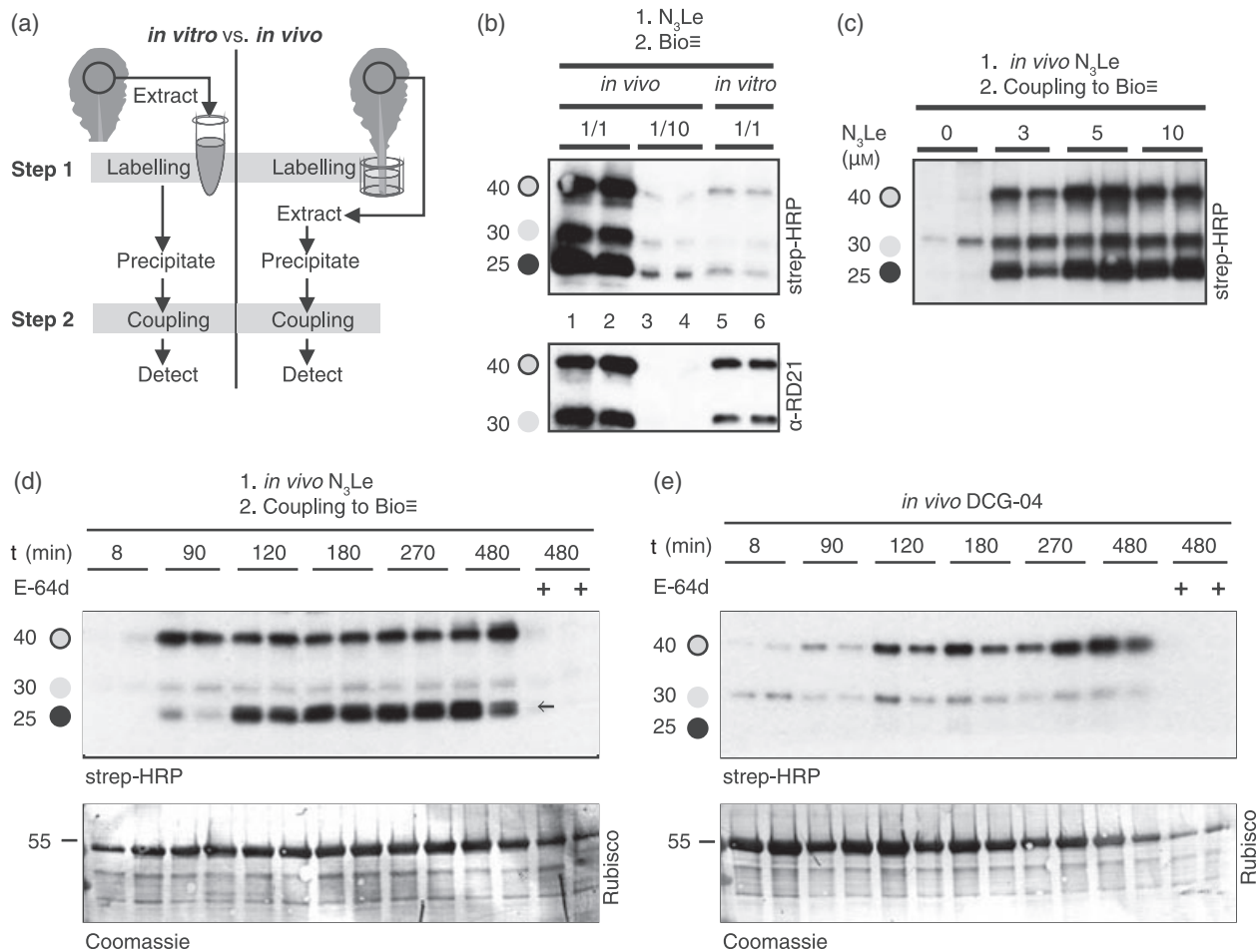


Figure 5. *In vivo* labelling with N_3Le and DCG-04.

(a) Schematic representation of the practical steps involved. *In vivo* labelling was achieved by incubating detached Arabidopsis leaves with their petioles in water containing N_3Le . After labelling, proteins were extracted from leaf discs (indicated with a circle) and coupled to Bio \equiv under denaturing conditions. (b) *In vivo* labelling with N_3Le is 10 times more efficient than *in vitro* labelling. Two Arabidopsis leaves from independent plants were incubated for 2 h with their petioles in solution containing 3 μM N_3Le (left). Simultaneously, proteins were extracted from two leaf discs of independent plants and labelled *in vitro* with 3 μM N_3Le . After labelling, protein extracts from both experiments were coupled with Bio \equiv and analysed as described in Figure 3(b). (c) *In vivo* labelling with different N_3Le concentrations. Leaves were incubated with 3, 5 and 10 μM N_3Le . After 2 h proteins were extracted from leaf discs and coupled with 6 μM Bio \equiv . Maximum labelling is reached if the leaves are incubated in a 5 μM N_3Le solution. (d), (e) Time course of *in vivo* labelling with N_3Le (d) and DCG-04 (e). Leaves were incubated in 10 μM N_3Le or 5 μM DCG-04. At different time-points leaf discs from two independently incubated leaves were taken and coupled with 6 μM Bio \equiv . Equal loading of proteins is shown by the corresponding Coomassie-stained blot (lower panel). Labelling occurs within 2 h, the right-most four lanes are less intense because of a staining error. Please note that the 25 kDa signal (arrow) is labelled by N_3Le but not by DCG-04.

permeable E-64d (Figure 5d, e, last lanes). In some cases, however, especially during longer incubation times, we could label 25-kDa signals with DCG-04, indicating that AALP labelling is conditional.

Previous identification of DCG-04 targets revealed that labelled proteins at 25 kDa include the Arabidopsis aleurain-like protease (AALP/AtAleu) (Van der Hoorn *et al.*, 2004). The AALP is localized in vacuoles (Ahmed *et al.*, Holwerda *et al.*, 1990), and is often used as a vacuolar marker protein (Heo *et al.*, 2005; Watanabe *et al.*, 2004). To investigate whether AALP is labelled by N_3Le , biotinylated proteins were purified on streptavidin magnetic beads and analysed on protein blots with anti-AALP antibodies. The signal at 25 kDa shows

that AALP is amongst the biotinylated proteins labelled by N_3Le , but significantly less by DCG-04 (Figure 6b, bottom panel), demonstrating that N_3Le labels the vacuolar protease AALP.

A candidate protease for causing signals at 30 and 40 kDa in N_3Le labelling is RD21. RD21 exists in two active isoforms: the 40-kDa intermediate isoform (iRD21) and the 30-kDa mature isoform (mRD21), which differ in the presence of a C-terminal propeptide (Yamada *et al.*, 2001). Both isoforms react with DCG-04 (Van der Hoorn *et al.*, 2004). Detection of purified biotinylated proteins with anti-RD21 antibody shows that the 40-kDa iRD21 and 30-kDa mRD21 isoforms are labelled by both N_3Le and DCG-04 (Figure 6b, top panel).

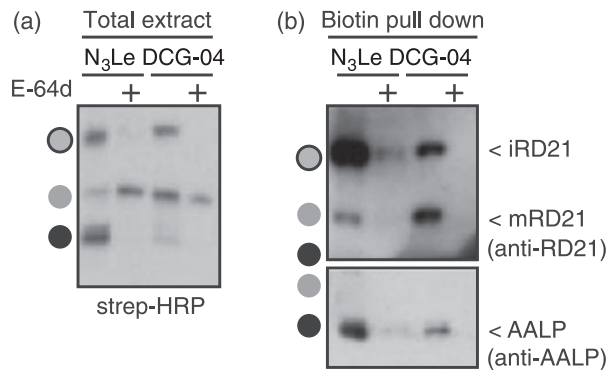


Figure 6. N₃Le labels the vacuolar protease AALP *in vivo*. Leaves were incubated in 5 μM N₃Le or 5 μM DCG-04 with or without 200 μM E-64d. N₃Le-labelled proteins were coupled with Bio≡. Biotinylated proteins were analysed on protein blot with streptavidin horseradish peroxidase (a), or purified on streptavidin beads and analysed on protein blot (b) with α-RD21 antibody (top) or α-AALP antibody (bottom). N₃Le can label AALP, whereas both probes label iRD21 and mRD21 *in vivo*.

Identifying targets of MVA178

To demonstrate the applicability of using click chemistry to identify targets of other small molecules, we used MVA178, a minitagged vinyl sulphone that targets the proteasome (Verdoes *et al.*, 2008). The proteasome resides in the cytoplasm and nucleus and is a large protein complex consisting of a regulatory 19S complex and a 20S core protease complex (Kurepa and Smalle, 2008). The catalytic β1, β2 and β5 subunits of the core protease of the proteasome are 23-kDa N-terminal nucleophile (Ntn) hydrolases that carry the catalytic Thr at the N-terminus of the mature protein. Although the role of the plant proteasome in selective degradation has been demonstrated in both defence and development studies (Sullivan *et al.*, 2003), the activity of the different catalytic subunits in living plant cells and their contributions to selective degradation remains to be investigated.

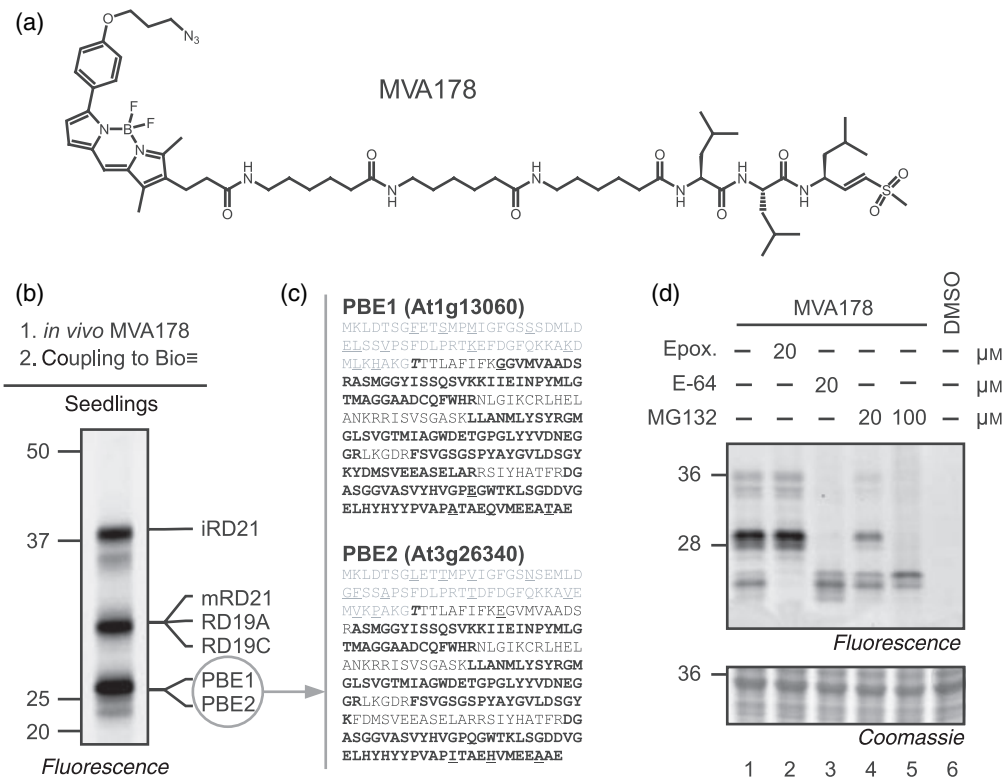


Figure 7. Identification of proteins labelled by vinyl sulphones *in vivo*.

(a) Structure of MVA178, an activity-based probe for the proteasome, containing a reactive group (vinyl sulfone, VS), a binding peptide (3 × Leu), a fluorescent reporter (BODIPY) and a minitag (azide).

(b) Identification of MVA178-labelled proteins using click chemistry. Seven-day-old seedlings were labelled with 2 μM MVA178 for 5 h. Proteins were extracted and azide-labelled proteins were coupled to Bio≡ using click chemistry under denaturing conditions. Labelled proteins were purified on streptavidin columns and separated on protein gels. Fluorescent signals were excised and proteins digested in-gel with trypsin. Eluted peptides were identified by liquid chromatography-tandem mass spectrometry (LC-MS/MS). Identified proteins are indicated on the right.

(c) Proteasome subunits identified by MS in the 25 kDa signal: grey, prodomain; **bold italic**, active site Thr; underlined, differences between PBE1 and PBE2; **bold**, identified peptides.

(d) Selective inhibition of MVA178 labelling *in vivo* using proteasome and Cys protease inhibitors. Arabidopsis cell cultures were pre-incubated for 30 min with epoxomycin (Epox), E-64 and MG132 at 20 or 100 μM, as indicated. Then, 2 μM MVA178 was added to the cultures to label the non-inhibited enzymes for 2 h. Proteins were extracted and separated on protein gels. Fluorescent proteins were visualized by fluorescence scanning. A representative of three independent experiments is shown.

MVA178 was recently used to study the proteasome in mammalian extracts (Verdoes *et al.*, 2008). MVA178 contains a vinyl sulfone reactive group, a peptide-binding group of three leucines, a long peptide-like linker, a fluorescent BODIPY reporter tag and an azide minitag (Figure 7a). To detect the targets of MVA178 in living plant cells, we incubated MVA178 with seedlings and cell cultures and detected fluorescent proteins on protein gels. This revealed three strong signals at 40, 30 and 23 kDa and weaker signals at 38 and 28 kDa (Figure 7b, d). Since we expected only signals at 23 kDa for the proteasome subunits, we were curious as to what other proteins become labelled by MVA178.

To reveal the identities of MVA178-labelled proteins, we coupled MVA178-labelled proteins with the Bio≡ reporter using click chemistry and purified the biotinylated proteins on streptavidin beads. However, during purification we noticed that copper ions cause massive protein precipitation and inactivation of streptavidin. We therefore adjusted the purification procedure by including EDTA to chelate copper and low concentrations of SDS to prevent protein precipitation (see Experimental Procedures). This resulted in an efficient purification of MVA178-labelled proteins from seedlings (Figure 7b). Purified MVA178-labelled proteins were separated on protein gels, and proteins in fluorescent bands were digested with trypsin and analysed by mass spectrometry (MS). This analysis demonstrated that the lower 23-kDa signal contains two β 5 subunits, PBE1 and PBE2 (Figure 7c). Unique peptides to both PBE1 (At1g13060) and PBE2 (At3g26340) were detected and the peptides covered the majority of the sequence of the mature proteins, except for the prodomain, which is removed during auto-activation, and the region containing the active site Thr, which is presumably labelled by MVA178 and becomes too large to be detected. Interestingly, proteins representing the other signals were identified as cysteine proteases RD21 (At1g47128) at 30 and 40 kDa, and RD19A (At4g39090) and RD19C (At4g16190) at 30 kDa (Table S1).

Studying selectivity of inhibitors *in vivo* using MVA178

Labelling of MVA178 to Arabidopsis cell cultures resulted in a similar labelling profile to labelling of seedlings (Figure 7d, lane 1). To confirm that the upper signals are papain-like cysteine proteases and the lower signals are proteasome subunits, we performed chemical interference assays using frequently used cell-permeable inhibitors that target papain-like cysteine proteases and the proteasome, respectively. As expected, pre-incubation with proteasome inhibitor epoxomicin prevents labelling of the 23-kDa signals but not the 30- and 40-kDa signals (Figure 7d, lane 2), whereas E-64d prevents labelling of the 30- and 40-kDa signals but not the 23-kDa signals (Figure 7d, lane 3). Interestingly, the presumed proteasome inhibitor MG132, which is most frequently used in plant research to study proteasome-

dependent processes, did not significantly inhibit labelling of the 23-kDa proteasome signals at 20 μ M, but suppressed the labelling of the 30- and 40-kDa signals (Figure 7d, lane 4). When used at 100 μ M, MG132 completely prevents labelling of the 30- and 40-kDa signals, but only partially suppressed labelling of the 23-kDa signal, whereas another signal at 24 kDa is induced (Figure 7d, lane 5). Similar data were generated by chemical interference assays on seedlings (data not shown). These data indicate that, when used *in planta*, MG132 acts as an inhibitor of papain-like cysteine proteases.

Discussion

In this report we established and validated a new two-step labelling procedure for small molecules in plants using minitags. To optimize the labelling parameters, we used the well-studied protease inhibitor E-64, which targets multiple proteases in plants, known to have different subcellular localizations. In contrast to biotinylated E-64, minitagged E-64 efficiently labels vacuolar proteases in living plant tissues. The two-step labelling procedure is applicable to a broad range of small molecules, as we illustrated with the minitagged vinyl sulphone.

The new coupling protocol differs from that introduced by Speers and Cravatt (2004). The original protocol requires reporter tag concentrations of 50–100 μ M, TCEP as the reducing agent and TBTA as the stabilizer of Cu⁺ (Chan *et al.*, 2004; Speers and Cravatt, 2004). We developed a coupling buffer that relies on DTT as the reducing agent and NaOAc as the buffer. In this buffer, TBTA was not required for coupling. Furthermore, coupling tolerates denaturing reagents (SDS and urea), ensuring that the observed profiles reflect *in vivo* conditions. Unspecific labelling is considerably reduced by using optimized reporter tag concentrations (3–10 μ M, Figure 4d). Furthermore, we added an acetone precipitation step before the coupling reaction to further standardize the procedure and we showed that 60 min is sufficient to achieve the coupling but that prolonged reaction times have no influence on unspecific labelling (Figure 4c). The protocol was slightly changed for the purification. In these large-scale experiments, the addition of TBTA was required for optimal labelling, acetone precipitation was omitted to prevent aggregation, and EDTA was added during purification to prevent Cu-induced protein precipitation and denaturation of streptavidin.

Besides using minitags for *in vivo* labelling, the two-step labelling procedure has a number of additional advantages. First, the synthesis of minitagged small molecules is significantly simplified when compared with biotin- or rhodamine-tagged small molecules. Minitagged reporters like Bio≡ can be synthesized in large quantities and used universally. Second, two-step labelling also facilitates more versatile detection methods since the reporter tags can be

chosen. Fluorescent reporter tags, for example, would allow quantitative, high-throughput detection. Third, when applied to fixed tissue, click chemistry could facilitate *in vivo* imaging of small-molecule targets. A similar *in vivo* imaging procedure has been used in medical research using Staudinger ligation (Hang *et al.*, 2006).

Using the coupling protocol we could investigate E-64 targets in living tissue. Profiles of N₃Le *in vivo* are similar but 10 times more intense when compared with *in vitro* labelling (Figure 5b). There may be different reasons for this increased reactivity. First, the investigated proteases could have been degraded during extraction and labelling. This assumption is consistent with decreased RD21 signal intensities on the immunoblot (Figure 5b). It is, however, also possible that the reduced labelling *in vitro* is caused by released endogenous protease inhibitors or loss of activators during extraction. Finally, the reactivity of the probe might be increased *in vivo*. The ethylester group in E-64 derivatives facilitates membrane permeability, but conversion of this group into a carboxyl group enhances inhibition (Powers *et al.*, 2002). It has been proposed that esterases catalyse this hydrolysis *in vivo* (Hang *et al.*, 2006), making N₃Le more active *in vivo* than *in vitro*.

In contrast to DCG-04, N₃Le labels the 25-kDa AALP protein. The AALP protein is often used as a vacuolar marker protein (Ahmed *et al.*, 2000), which indicates that N₃Le passes through membranes. This conclusion is strengthened by the slower N₃Le labelling rate of the 25-kDa protein when compared with the 40-kDa signal (Figures 5d, e). DCG-04 does not label AALP, consistent with the notion that DCG-04 is not membrane permeable (Lennon-Dumenil *et al.*, 2002). However, we found that some labelling of AALP by DCG-04 can occur, especially after prolonged incubation times or if materials and conditions are varied (data not shown).

DCG-04 labels the 40-kDa intermediate (i) isoform of RD21 *in vivo* (Figure 6, Yamada *et al.*, 2001), indicating that this is a secreted protease. RD21 secretion is consistent with the identification of the tomato RD21 orthologue C14 in apoplastic fluids (Shabab *et al.*, 2008). However, the labelling of 40-kDa iRD21 with N₃Le is stronger, indicating that most of the iRD21 is in vesicles. This is consistent with immunolocalization studies, which showed that RD21 localizes in vesicles that originate from the endoplasmic reticulum (ER-bodies; Hayashi *et al.*, 2001). The slower labelling of the 40-kDa iRD21 by DCG-04 when compared with N₃Le (Figure 5d, e) could result from a lower diffusion rate of the larger DCG-04.

Studies with MVA178 revealed that this molecule reacts with proteasome subunits PBE1 and PBE2. The fact that both these β 5 subunits reacted with MVA178 indicates that both are active in seedlings. The β 1 and β 2 catalytic subunits (PBA1, PBB1 and PBB2) were not detected in this assay, but were detected in other assays (C. Gu, J. Misas-Villamil and RvdH, MPIZ, Cologne, DE, unpublished results). Besides proteasome subunits, MVA178 also labels papain-like

cysteine proteases RD21 and RD19A and RD19B. Since this labelling can be prevented by adding E-64, we conclude that this labelling is not caused by off-target labelling by click chemistry but by MVA178 labelling itself. Although unexpected, papain-like cysteine proteases are known to be irreversibly inhibited by vinyl sulfones, especially if they carry a Leu at the P2 position (Powers *et al.*, 2002). We could also detect RD19 proteases using activity-based probes. RD19A is a vesicle-localized protease that was recently found to accumulate in the nucleus upon co-expression with the bacterial type-III effector PopP2 (Bernoux *et al.*, 2008). The two-step labelling method can be used to study the activity of RD19 in the presence of PopP2 in living tissue.

By knowing the targets of MVA178, we could monitor their activities in living cells and test the selectivity of frequently used inhibitors. This demonstrated that epoxomycin and E-64d selectively inhibit their expected target enzymes in living cells. The presumed proteasome inhibitor MG132, however, also inhibits cysteine proteases. These data are consistent with data generated using animal cysteine proteases (Lee and Goldberg, 1998). MG132 is the most frequently used proteasome inhibitor in plant science, and MG132-induced phenotypes were often explained to be caused by proteasome inhibition, for example in xylogenesis, auxin signalling and defence (Zhao *et al.*, 2008; Laxmi *et al.*, 2008; Chini *et al.*, 2007). The data presented here indicate that special care should be taken to interpret MG132 data and that it is better to use epoxomycin for chemical interference studies. MG132 could not prevent labelling of the proteasome by MVA178 under these conditions, but this does not exclude that it inhibits the proteasome since MG132 is a reversible inhibitor that may not be able to prevent labelling by the irreversible MVA178 probe over prolonged incubation times.

Application of the two-step labelling protocol is not only restricted to the visualization of Cys proteases and the proteasome but it is significantly broader. In medical research, the two-step click-chemistry procedure has been used by Cravatt and co-workers to identify other small-molecule targets, including glycosidases, histone deacetylases, metalloproteases and cytochrome P450s (reviewed by Cravatt *et al.*, 2008). Some of these activity-based probes were based on reversible inhibitors that were made irreversible by adding a photoreactive group. Another field of application concerns studies on post-translational modification by feeding experiments with minitagged precursors to reveal, for example, myristoylated or glycosylated proteins (Hang *et al.*, 2007; Prescher *et al.*, 2004). When combined with photoreactive groups, this two-step labelling procedure might also be useful for identifying the targets of phytohormones, herbicides and small molecules selected by chemical genetic screens. Quantification of click-chemistry labelled proteins can be done if fluorescent reporter tags are used. Quantification by mass spectrometry requires special

quantification techniques like spectral counting, iTRAQ or isotope labelling (Thelen and Peck, 2007).

We used the two-step labelling procedure to study small-molecule targets in detached leaves, seedlings and cell cultures. It seems likely that the applications can be expanded to study other tissues like seeds, roots and siliques, and to other plant species. When applied to the study of biological processes, these procedures might reveal biochemical processes that have never been noticed before. For example, using small-molecule probes we found that defence-related, diversifying cysteine proteases of tomato are specifically inhibited by a fungal effector protein (Shabab *et al.*, 2008), and that Arabidopsis extracts contain a papain-like peptide ligase (Wang *et al.*, 2008). Taken together, the application of this two-step labelling procedure will greatly advance our understanding of how small molecules modify and mediate the biological functions of plants.

Experimental procedures

Plant materials and antibodies

Arabidopsis thaliana ecotype Columbia was grown in a normal greenhouse at 22°C under a 16-h light regime. Leaves were taken from 4–5-week-old plants. Antibodies for detection of RD21 and AALP were kindly provided by Dr C. MacKintosh (MRC, University of Dundee, UK) and Dr N. Raikhel (CEPCEB, Riverside, CA, USA), respectively. Horseradish peroxidase-conjugated anti-sheep antibodies were from Santa Cruz Biotechnology (<http://www.scbt.com/>) and anti-rabbit antibodies were from Amersham Pharmacia Biotech (<http://www.amersham.com>).

Organic synthesis

All synthesized compounds are available upon request. DCG-04, BioRhN₃ and MVA178 were synthesized as described previously (Greenbaum *et al.*, 2000; Speers and Cravatt, 2004; Verdoes *et al.*, 2008). Solvents used in the solid phase peptide synthesis, *N,N*-diisopropylethylamine (DiPEA) and trifluoroacetic acid (TFA) were all of peptide synthesis grade (Biosolve, <http://www.biosolve-chemicals.com>) and used as-received. The protected amino acids, Rink amide MBHA resin (0.78 mmol g⁻¹) and HCTU (2-(6-chloro-1H-benzotriazole-1-yl)-1,1,3,3-tetramethyl aluminium hexafluorophosphate) were obtained from NovaBiochem. Solid-phase peptide synthesis (SPPS) was carried out using a 180° Variable Rate Flask Shaker (St John Associates, Inc., <http://www.stjohnassociates.com/>). Liquid chromatography (LC)/MS analysis was performed on a Jasco HPLC system (detection simultaneously at 214 and 254 nm) coupled to a Perkin Elmer Sciex API 165 mass spectrometer equipped with a custom-made electrospray interface (ESI). An analytical Alltima C₁₈ column (Alltech, <http://www.alltech.com/>; 4.6 mm × 250 mm, 5 µm particle size) was used. Buffers were: A = H₂O; B = CH₃CN; C = 0.5% aq TFA. For reverse phase (RP) HPLC purification of N₃YL_e (PS334) and N₃Le (PS472) a Biocad 'Vision' automated HPLC system (Applied Biosystems, <http://www.appliedbiosystems.com>) was used. The applied buffers were A, B and C. The ¹H-NMR spectra were recorded with a Bruker AC200 instrument at 200 MHz with chemical shifts (δ) relative to tetramethylsilane.

≡YL_e (SV38) was synthesized on polystyrene-based Rink resin, following standard 9-fluorenylmethyloxycarbonyl (Fmoc) solid

phase peptide synthesis protocols. In brief, Fmoc removal took place by using 20% piperidine in dimethylformamide (DMF). The Fmoc-protected amino acids (3 eq.) were coupled under influence of a combination of diisopropylcarbodiimide (DIC; 3 eq.) and hydroxybenzotriazole (HOBt; 3 eq.) in DMF. In this way, Fmoc-propargylglycine, Fmoc-aminohexanoic acid, Fmoc-tyrosine and Fmoc-leucine were coupled. After final Fmoc deprotection, the terminal amino functionality was capped with the reactive group using an activated nitrophenyl ester derivative of the epoxysuccinate, as previously described (Verhelst and Bogoy, 2005). The probe was cleaved from the solid support by reaction with TFA/H₂O/triisopropylsilane (TIS) (18/1/1) for 1 h. The cleavage solution was evaporated to dryness and purified by reverse phase HPLC, yielding ≡YL_e as a fluffy white solid. Liquid chromatography/MS (ESI), [M + H]⁺ calculated for C₃₂H₄₆N₅O₉ 644.3, found 644.5; [M + Na]⁺ calculated 666.3, found 666.5.

≡Le (SV49) was synthesized as follows: ethyl(2*S*, 3*S*)-oxirane-2,3-dicarboxylate (160 mg, 1 mmol) was dried by co-evaporation with toluene, dissolved in THF (5 ml) and cooled to -10°C. Subsequently, isobutylchloroformate (144 µl, 1.1 mmol) and *N*-methylmorpholine (121 µl, 1.2 mmol) were added and the reaction mixture was stirred for 25 min. Leucine *tert*-butyl ester (224 mg, 1 mmol) and *N*-methylmorpholine (242 µl, 2.4 mmol) were added, and the reaction was stirred until TLC analysis (ethyl acetate, EtOAc) revealed full conversion of the starting materials. The reaction mixture was diluted with EtOAc, washed with 1 M hydrochloric acid, sat. bicarbonate and brine. The organic layer was dried on MgSO₄ and concentrated under reduced pressure. The residue was dissolved in TFA/dichloromethane (DCM) 1/1, stirred for 1 h and concentrated with co-evaporation from toluene. Diisopropyl ethyl amine (DIEA; 212 µl, 1.2 mmol) was added to a solution of the crude free acid in tetrahydrofuran (THF; 4 ml). The solution was cooled to -10°C, after which isobutylchloroformate (144 µl, 1.1 mmol) was added. The reaction mixture was stirred for 30 min before propargylamine hydrochloride (92 mg, 1 mmol) and DIEA (212 µl, 1.2 mmol) were added. After TLC analysis (EtOAc/hexane 1/1) revealed completion of the reaction, the same work-up procedure was followed as described for the first coupling reaction. Silica column chromatography [0–5% methanol (MeOH) in DCM] afforded the title compound as a white solid (191 mg, 62% yield over three steps). Liquid chromatography/MS (ESI): [M + H]⁺ calculated for C₁₅H₂₃N₂O₅ 311.2, found 311.2; [M + Na]⁺ calculated 333.1, found 333.2. ¹H NMR (500 MHz): 7.10 (t, 1H, *J* = 5.0 Hz), 7.00 (d, 1H, *J* = 8.8 Hz), 4.61–4.54 (m, 1H), 4.31–4.22 (m, 2H), 4.03 (dd, 2H, *J* = 5.1 Hz, *J* = 2.5 Hz), 3.75 (d, 1H, *J* = 1.8 Hz), 3.52 (d, 1H, *J* = 1.8 Hz), 2.25 (t, 1H, *J* = 2.5 Hz), 1.68–1.54 (m, 2H), 1.32 (t, 3H, *J* = 7.1 Hz), 0.94 (d, 3H, *J* = 6.2 Hz), 0.91 (d, 3H, *J* = 6.2 Hz). ¹³C NMR (125 MHz): 171.0, 166.6, 166.2, 79.0, 71.8, 62.3, 53.7, 52.8, 51.1, 41.2, 29.2, 24.7, 22.8, 22.0, 14.0.

N₃Le (PS472): *tert*-butyloxycarbonyl-leucine (Boc-Leu-OH) hydrate (715 mg, 2.9 mmol) was co-evaporated (toluene, 3 ×) and dissolved in THF (10 ml) at 0°C under N₂ atmosphere. Isobutyl chloroformate (448 mg, 3.3 mmol) and triethylamine (Et₃N; freshly distilled, 0.46 ml, 3.3 mmol) were added. The mixture was stirred for 5 min and filtered into a solution of 1-azido-4-aminobutane (Lee *et al.*, 2001) (250 mg, 2.2 mmol) in THF (5 ml) and was stirred for 1.5 h until TLC analysis (hexanes/EtOAc 1/1 v/v) indicated a completed reaction. The mixture was diluted (EtOAc, 50 ml), washed (1 N aq. HCl 2 × 30 ml, sat. aq. NaHCO₃ 2 × 30 ml, sat. aq. NaCl 2 × 30 ml), dried over MgSO₄, filtered and concentrated *in vacuo*. The crude product was purified by silica chromatography (hexanes/EtOAc 6/1 to 3/1 v/v) to yield 515 mg (1.6 mmol, 72%) of *tert*-butyloxycarbonyl-leucine-*tert*-butylester (Boc-Leu-Bu)-N₃, which was dissolved in TFA/CH₂Cl₂ (10 ml, 1/1 v/v) for 1 h. The mixture was concentrated *in vacuo*, co-evaporated (toluene, 3 ×) and

dissolved in THF (5 ml). In a separate flask, ethyl (2S,3S)oxirane-2,3-dicarboxylate (460 mg, 2.9 mmol) was treated with isobutyl chloroformate (448 mg, 3.3 mmol) and Et₃N (freshly distilled, 0.46 ml, 3.3 mmol) in THF (10 ml) at 0°C under N₂ atmosphere for 5 min and filtered into the H-Leu-Bu-N₃ solution. The mixture was stirred for 2 h, diluted (EtOAc, 50 ml), washed (1 N aq. HCl 2 × 30 ml, sat. aq. NaHCO₃ 2 × 30 ml, sat. aq. NaCl 2 × 30 ml), dried over MgSO₄, filtered and concentrated *in vacuo*. The crude product was purified by silica chromatography (hexanes/EtOAc 4/1 to EtOAc) to yield 300 mg (0.8 mmol, 52% of the title compound). ¹H NMR (CDCl₃): δ, 6.83 (d, 1H, *J* = 8.4 Hz), 6.52–6.38 (m, 1H), 4.48–4.34 (m, 1H), 4.32–4.21 (m, 2H), 3.70 (d, 1H, *J* = 1.8 Hz), 3.49 (d, 1H, *J* = 1.8 Hz), 3.35–3.24 (m, 4H), 1.64–1.50 (m, 5H), 1.32 (t, 3H, *J* = 7.2 Hz), 0.96–0.90 (m, 8H). LC/MS [M + H]⁺ calculated for C₁₆H₂₇N₅O₅: 370.4, found 370.4.

N₃YLe (PS334): Fmoc-protected Rink amide resin (78 mg, 50 μmol) was elongated by standard Fmoc-based SPPS to give resin-bound Lys(N₃)-Ahx-Tyr-Leu-epoxirane. In brief, where appropriate removal of the Fmoc protecting group was accomplished by treatment of the resin-bound peptide with 20% (v/v) piperidine in *N*-methylpyrrolidone (NMP) for 20 min. Peptide-coupling steps were performed by treatment of the resin with a pre-mixed (5 min) solution of the appropriate acid (5 eq.), HCTU (5 eq.) and DiPEA (6 eq.) in NMP (0.5 ml) for 1 h unless stated otherwise. Coupling efficiencies were monitored with the Kaiser test and couplings were repeated if necessary. After coupling and deprotecting steps the resin was washed with NMP (5 ×). After the last coupling step, the resin was washed extensively (alternating CH₂Cl₂-MeOH 3 ×, alternating CH₂Cl₂-Et₂O 3 ×), transferred into a clean vial and treated with TFA/H₂O/TIS (1 ml, 95/2.5/2.5 v/v/v) for 1 h. The mixture was filtered and the resin washed with TFA (2 × 1 ml). The filtrate was diluted (toluene, 10 ml) and concentrated *in vacuo*. The crude product was co-evaporated (toluene, 3 ×) and purified to homogeneity by RP-HPLC, applying a linear gradient (33–40% B in three column volumes) to yield 7 mg (9 μmol, 18%) of the title compound. Liquid chromatography/MS [M + H]⁺ calculated for C₃₃H₅₀N₈O₉: 704.4, found 704.6.

Bio≡ (PS446): To a solution of biotin (244 mg, 1 mmol) in DMF (10 ml) was added *N*-hydroxysuccinimide (HOSu) (140 mg, 1.2 mmol) and DIC (180 μl, 1.2 mmol) and the reaction mixture was stirred overnight. Propargyl amine (82 μl, 1.2 mmol) was added and the mixture was stirred overnight. The solvents were evaporated *in vacuo*, and the product was purified to homogeneity by silica gel chromatography (CH₂Cl₂/MeOH 19/1 to 9/1 v/v) to yield 200 mg (0.7 mmol, 71%) of the title compound. ¹H NMR (CD₃OD): δ, 4.43–4.36 (m, 1H), 4.24–4.17 (m, 1H), 3.85 (d, 2H, *J* = 2.7 Hz), 3.16–3.05 (m, 1H), 2.83 (dd, 1H, *J* = 12.4 Hz, *J* = 4.5 Hz), 2.60 (d, 1H, *J* = 12.4 Hz), 2.47 (t, 1H, *J* = 2.6 Hz), 2.12 (t, 2H, *J* = 7.3 Hz), 1.63–1.30 (m, 6H). Liquid chromatography/MS [M + H]⁺ calculated C₁₃H₁₉N₃O₂S: 282.2, found 282.3.

Two-step labelling procedure

Proteins from one *Arabidopsis* leaf were extracted by grinding the leaf in an Eppendorf tube with 1 ml water. The extracts were cleared by centrifugation (1 min, 16 000 *g*). 450 μl of supernatant was transferred to a fresh Eppendorf tube and supplemented with 50 μl 10 × labelling buffer (250 mM NaOAc, 10 mM L-cysteine) and 3–10 μM probe. In control reactions a 10 to 20 times molar excess of E-64 (Sigma, <http://www.sigmaaldrich.com/>) was added to compete for specific labelling. The reaction was incubated for 5 h and the proteins were precipitated with 1 ml cold acetone. Precipitated proteins were dissolved in 500 μl coupling buffer (50 mM NaOAc pH 6, 1 mM CuSO₄, 1% SDS, 3–6 μM BioRhN₃/Bio≡ and 0.4 mM fresh DTT). Samples were incubated at room temperature for 1 h and the

reaction was stopped by adding 1 ml cold acetone. Precipitated proteins were redissolved in 2 × SDS-PAGE gel loading buffer, separated on a 12–16% SDS polyacrylamide gel (Sambrook and Russell, 2001) and transferred to a protein membrane. Biotinylated proteins were detected with streptavidin-HRP (1:3000, Ultrasensitive, Sigma) and chemiluminescence (ECL, Pierce, <http://www.piercenet.com/>).

In vivo labelling of leaves with N₃Le

Leaves were incubated with their petioles in a solution containing 3–5 μM N₃Le with or without 100–200 μM E-64d (Sigma). After 2 h, 0.5 cm² leaf discs were punched out and proteins extracted by grinding the leaf in an Eppendorf tube in 600 μl water, 1% SDS or 6 M urea. The extracts were cleared by centrifugation and 500 μl of the supernatant was transferred to a fresh Eppendorf tube. Proteins were precipitated with 1 ml cold acetone and subjected to the coupling protocol and analysed as described above. For the *in vivo* time course, two leaves per time point were incubated in a solution containing 10 μM N₃Le. After each time point two independent leaf discs were excised, transferred to Eppendorf tubes and frozen at –20°C. At the end of the time course all samples were processed as described above. For affinity purification, biotinylated proteins were captured on magnetic streptavidin beads (Promega, <http://www.promega.com/>), washed twice with 1% SDS in TRIS-buffered saline Tween-20 (TBST) and twice with 6 M urea in TBST, boiled in SDS sample buffer and detected on protein blots with anti-AALP and anti-RD21 antibodies.

Identification of MVA178-labelled proteins from seedlings

Seedlings (ecotype Columbia) were grown for 7 days in a climate chamber on MS-agar medium. Forty seedlings were submerged in 500 μl 2 μM MVA178 for 5 h in the dark. The seedlings were washed with water and proteins were extracted in 500 μl water. The protein extract was cleared by centrifugation [13 000 *g*, 1 min, room temperature (RT) (22–24°C)] and proteins in the supernatant were precipitated with two volumes of ice-cold acetone. The pellet was briefly washed with 300 μl ice-cold 70% acetone. The pellet was dried for 5 min and dissolved in 1% SDS to a final protein concentration of 1 mg ml⁻¹. One millilitre of this protein solution was supplemented with 50 μl 1 M sodium acetate pH 6, 10 μl 1 mM Bio≡, 20 μl 50 mM CuSO₄ and 20 μl 1.7 mM TBTA [Sigma, 678937, dissolved in *t*-butyl alcohol (*t*-BuOH):H₂O 1:4]. The solution was vortexed briefly after addition of each component. Finally the click chemistry reaction was started by adding 10 μl 100 mM TCEP (Sigma, 98284, final ~1 mM). The reaction was stopped after 1 h by adding 10 μl 500 mM EDTA. The reaction mix was diluted with 1.5 ml phosphate-buffered saline (PBS, Gibco, <http://www.invitrogen.com>) and loaded onto a PD-10 (Amersham, <http://www.amersham.com>) desalting column pre-equilibrated with PBS. Proteins were eluted with 3.5 ml of 1 × PBS. The collected flow through was further diluted with 5 ml PBS and supplemented with 100 μl 10% SDS. Biotinylated proteins were captured by adding 100 μl avidin beads (Sigma, A-9207, washed three times with 1 ml PBS) and inverting the tubes for 1 h at RT. The beads were collected by centrifugation (5 min, 1400 *g*) and washed six times with 10 ml 1% SDS. Captured proteins were released from the matrix by heating the beads at 90°C for 5 min in 50 μl gel-loading buffer. The samples were briefly centrifuged and 35–50 μl of the supernatant loaded on a 10% protein gel. Labelled proteins were visualized by fluorescence and then excised. Gel slices were treated with trypsin and eluted peptides analysed by a Thermo Scientific LTQ-XL as follows: a 10 cm capillary (100 μm diameter) was loaded with C18

and equilibrated with buffer A (5% acetonitrile, 0.1% formic acid in water). Peptides were loaded in 5 µl 0.1% formic acid solution and eluted for 2 h using a gradient from 100% buffer A to 20% buffer A/80% buffer B (buffer B: 50% acetonitrile, 0.1% formic acid in water). Spectra were collected and analysed using SEQUEST 3.0 (Tabb *et al.*, 2002) using the Arabidopsis EPI-IPI 2007 protein database allowing all possible cleavage sites. A reverse sequence database was included as negative control. Positive hits were selected by DTaselect v2.0.26 (Tabb *et al.*, 2002) by only accepting a minimum of two peptides per protein.

Labelling cell cultures with MVA178

Cell cultures (Arabidopsis ecotype Landsberg; May and Leaver, 1993) were weekly subcultured in medium [3% w/v sucrose, 0.5 mg L⁻¹ naphthalene acetic acid, 0.05 mg L⁻¹ 6-benzylaminopurine (BAP) and 4.4 g MS Gamborg B₅ vitamins (Duchefa, <http://www.duchefa.com/>), pH 5.7]. Before labelling, 6 ml of the medium of a 7-day-old cell culture was replaced by fresh medium. One hundred microliters of cell culture was pre-incubated for 30 min with inhibitors and then labelled for 2 h in the dark with 2 µM MVA178. Cells were harvested by centrifugation (1 min, 16 000 g) and washed once with 100 µl of medium. Proteins were extracted from cells by grinding the pellet in 100 µl of distilled water. The extract was cleared by centrifugation and the supernatant was mixed with 25 µl of a 4 × SDS-PAGE buffer. The samples were then heat denatured (95°C, 5 min) and proteins separated on a 12% protein gel. Fluorescently labelled signals were detected using a Typhoon scanner (Molecular Dynamics, <http://www.amersham.com>, ex 532 nm, em 583 nm BP30).

Acknowledgements

We are grateful to Dr Benjamin F. Cravatt, Dr Sherry Niessen, Heather Hoover (Scripps Institute, San Diego, USA) and Dr Bobby Florea (Leiden University, Netherlands) for their help with mass spectrometry, Dr Carol MacKintosh (MRC, University of Dundee, UK) and Dr Natasha Raikhel (CEPCEB, Riverside, CA, USA), for providing the RD21 and AALP-antibody, respectively, Dr Scott Peck for providing the Arabidopsis cell cultures; Johana Misas for help with cell cultures experiments, Koumis Philippou and Izabella Kolodziejek for providing seedlings, and Christian Gu and Dr Michiel Leeuwenburgh for useful suggestions. This work was supported by the Max Planck Society and the Deutsche Forschungsgemeinschaft (DFG project HO 3983/3–3).

Supporting Information

Additional Supporting Information may be found in the online version of this article:

Table S1. Mass spectroscopic data for MVA178-labelled proteins. Please note: Wiley-Blackwell are not responsible for the content or functionality of any supporting materials supplied by the authors. Any queries (other than missing material) should be directed to the corresponding author for the article.

References

Ahmed, S.U., Rojo, E., Kovaleva, V., Venkataraman, S., Dombrowski, J.E., Matsuoka, K. and Raikhel, N.V. (2000) The plant vacuolar sorting receptor AtELP is involved in transport of NH(2)-terminal

propeptide-containing vacuolar proteins in Arabidopsis thaliana. *J. Cell Biol.* **149**, 1335–1344.

- Bernoux, M., Timmers, T., Jauneau, A., Brière, C., De Wit, P.J.G.M., Marco, Y. and Deslandes, L. (2008) RD19, an Arabidopsis cysteine protease required for RRS1-R-mediated resistance, is relocalized to the nucleus by the *Ralstonia solanacearum* PopP2 Effector. *Plant Cell*. in press.
- Chan, T.R., Hilgraf, R., Sharpless, K.B. and Fokin, V.V. (2004) Polytriazoles as copper(I)-stabilizing ligands in catalysis. *Org. Lett.* **6**, 2853–2855.
- Chini, A., Fonseca, S., Fernandez, G. *et al.* (2007) The JAZ family of repressors is the missing link in jasmonate signalling. *Nature*, **448**, 666–671.
- Cravatt, B.F., Wright, A.T. and Kozarich, J.W. (2008) Activity-based protein profiling: from enzyme chemistry to proteomic chemistry. *Ann. Rev. Biochem.* **77**, 383–414.
- Greenbaum, D., Medzihradsky, K.F., Burlingame, A. and Bogoy, M. (2000) Epoxide electrophiles as activity-dependent cysteine protease profiling and discovery tools. *Chem. Biol.* **7**, 569–581.
- Hang, H.C., Loureiro, J., Spooner, E., van der Velden, A.W., Kim, Y.M., Pollington, A.M., Maehr, R., Starnbach, M.N. and Ploegh, H.L. (2006) Mechanism-based probe for the analysis of cathepsin cysteine proteases in living cells. *ACS Chem. Biol.* **1**, 713–723.
- Hang, H.C., Geutjes, E.J., Grotenbreg, G., Pollington, A.M., Bijlmakers, M.J. and Ploegh, H.L. (2007) Chemical probes for the rapid detection of fatty-acylated proteins in mammalian cells. *J. Am. Chem. Soc.* **129**, 2744–2745.
- Hayashi, Y., Yamada, K., Shimada, T., Matsushima, R., Nishizawa, N.K., Nishimura, M. and Hara-Nishimura, I. (2001) A proteinase-storing body that prepares for cell death or stresses in the epidermal cells of Arabidopsis. *Plant Cell Physiol.* **42**, 894–899.
- Heo, J.B., Rho, H.S., Kim, S.W., Hwang, S.M., Kwon, H.J., Nahm, M.Y., Bang, W.Y. and Bahk, J.D. (2005) OsGAP1 functions as a positive regulator of OsRab11-mediated TGN to PM or vacuole trafficking. *Plant Cell Physiol.* **46**, 2005–2018.
- Holwerda, B.C., Galvin, N.J., Baranski, T.J. and Rogers, J.C. (1990) *In vitro* processing of aleurain, a barley vacuolar thiol protease. *Plant Cell*, **2**, 1091–1106.
- Huisgen, R. (1984). Introduction, survey, mechanism. In *1,3-Dipolar Cycloaddition Chemistry* (Padwa, A., ed.). New York: Wiley, pp. 1–176.
- Kaschani, F. and Van der Hoorn, R. (2007) Small molecule approaches in plants. *Curr. Opin. Chem. Biol.* **11**, 88–98.
- Kolb, H.C., Finn, M.G. and Sharpless, K.B. (2001) Click chemistry: diverse chemical function from a few good reactions. *Angew. Chem. Int. Ed.* **40**, 2004–2021.
- Kurepa, J. and Smalle, J.A. (2008) Structure, function and regulation of plant proteasomes. *Biochimie*, **90**, 324–335.
- Laxmi, A., Pan, J., Morsy, M. and Chen, R. (2008) Light plays an essential role in intracellular distribution of auxin efflux carrier PIN2 in Arabidopsis thaliana. *PLoS ONE*, **3**, e1510.
- Lee, D.H. and Goldberg, A.L. (1998) Proteasome inhibitors: valuable tools for cell biologists. *Trends Cell Biol.* **8**, 387–403.
- Lee, J.W., Jun, S.I. and Kim, K. (2001) An efficient and practical method for the synthesis of mono-N-protected α,ω -diaminoalkanes. *Tetrahedron Lett.* **42**, 2709–2711.
- Lennon-Dumenil, A.M., Bakker, A.H., Maer, R., Fiebiger, E., Overkleeft, H.S., Roseblatt, M., Ploegh, H.L. and Lagaudriere-Gesbert, C. (2002) Analysis of protease activity in live antigen-presenting cells shows regulation of the phagosomal proteolytic contents during dendritic cell activation. *J. Exp. Med.* **196**, 529–539.

- May, M.J. and Leaver, C.J.** (1993) Oxidative stimulation of glutathione synthesis in *Arabidopsis thaliana* suspension cultures. *Plant Physiol.* **103**, 621–627.
- Powers, J.C., Asgian, J.L., Ekici, O.D. and James, K.E.** (2002) Irreversible inhibitors of serine, cysteine, and threonine proteases. *Chem. Rev.* **102**, 4639–4750.
- Prescher, J.A., Dube, D.H. and Bertozzi, C.R.** (2004) Chemical remodelling of cell surfaces in living animals. *Nature*, **430**, 873–877.
- Rostovtsev, V.V., Green, L.G., Fokin, V.V. and Sharpless, K.B.** (2002) A stepwise Huisgen cycloaddition process: copper(I)-catalyzed regioselective “ligation” of azides and terminal alkynes. *Angew. Chem. Int. Ed. Engl.* **41**, 2596–2599.
- Sambrook, J. and Russell, D.W.** (2001) *Molecular Cloning: A Laboratory Manual*, 3rd edn. New York: Cold Spring Harbor Laboratory Press.
- Shabab, M., Shindo, T., Gu, C., Kaschani, F., Pansuriya, T., Chintha, R., Harzen, A., Colby, T., Kamoun, S. and Van der Hoorn, R.A.L.** (2008) Fungal effector protein AVR2 targets diversifying defence-related Cys proteases of tomato. *Plant Cell*, **20**, 1169–1183.
- Speers, A.E. and Cravatt, B.F.** (2004) Profiling enzyme activities *in vivo* using click chemistry methods. *Chem. Biol.* **11**, 535–546.
- Sullivan, J.A., Shirasu, K. and Deng, X.W.** (2003) The diverse roles of ubiquitin and the 26S proteasome in the life of plants. *Nature Rev. Genet.* **4**, 948–958.
- Tabb, D.L., McDonald, W.H. and Yates, J.R. 3rd** (2002) DTASelect and contrast: tools for assembling and comparing protein identifications from shotgun proteomics. *J. Proteome Res.* **1**, 21–26.
- Thelen, J.J. and Peck, S.C.** (2007) Quantitative proteomics in plants: choices in abundance. *Plant Cell*, **19**, 3339–3346.
- Tornøe, C.W., Christensen, C. and Meldal, M.** (2002) Peptidotriazoles on solid phase: [1,2,3]-triazoles by regioselective copper(I)-catalyzed 1,3-dipolar cycloadditions of terminal alkynes to azides. *J. Org. Chem.* **67**, 3057–3064.
- Van der Hoorn, R.A., Leeuwenburgh, M.A., Bogyo, M., Joosten, M.H. and Peck, S.C.** (2004) Activity profiling of papain-like cysteine proteases in plants. *Plant Physiol.* **135**, 1170–1178.
- Verdoes, M., Florea, B.I., Hillaert, U., Willems, L.I., Van der Linden, W.A., Saeheng, M., Filippov, D.V., Kisselev, A.F., Van der Marel, G.A. and Overkleeft, H.S.** (2008) Azido-BODIPY acid reveals quantitative Staudinger-Bertozzi ligation in two-step activity-based proteasome profiling. *ChemBioChem*, **9**, 1735–1738.
- Verhelst, S.H.L. and Bogyo, M.** (2005) Solid-phase synthesis of double-headed epoxysuccinyl activity-based probes for selective targeting of papain family cysteine proteases. *Chembiochem*, **6**, 824–827.
- Wang, Q., Chan, T.R., Hilgraf, R., Fokin, V.V., Sharpless, K.B. and Finn, M.G.** (2003) Bioconjugation by copper(I)-catalyzed azide-alkyne [3 + 2] cycloaddition. *J. Am. Chem. Soc.* **125**, 3192–3193.
- Wang, Z., Gu, C., Colby, T., Shindo, T., Balamurugan, R., Waldmann, H., Kaiser, M. and Van der Hoorn, R.A.L.** (2008) β -lactone probes identify a papain-like peptide ligase in *Arabidopsis thaliana*. *Nat. Chem. Biol.* **4**, 557–563.
- Watanabe, E., Shimada, T., Tamura, K., Matsushima, R., Koumoto, Y., Nishimura, M. and Hara-Nishimura, I.** (2004) An ER-localized form of PV72, a seed-specific vacuolar sorting receptor, interferes the transport of an NPIR-containing proteinase in *Arabidopsis* leaves. *Plant Cell Physiol.* **45**, 9–17.
- Yamada, K., Matsushima, R., Nishimura, M. and Hara-Nishimura, I.** (2001) A slow maturation of a cysteine protease with a granulin domain in the vacuoles of senescing *Arabidopsis* leaves. *Plant Physiol.* **127**, 1626–1634.
- Zhao, C., Avci, U., Grant, E.H., Haigler, C.H. and Beers, E.P.** (2008) XND1, a member of the NAC domain family in *Arabidopsis thaliana*, negatively regulates lignocellulose synthesis and programmed cell death in xylem. *Plant J.* **53**, 425–436.